

Scaling and self-averaging in the three-dimensional random-field Ising model

N.G. Fytas^a and A. Malakis

Department of Physics, Section of Solid State Physics, University of Athens, Panepistimiopolis, GR 15784 Zografos, Athens, Greece

Received: date / Revised version: date

Abstract. We investigate, by means of extensive Monte Carlo simulations, the magnetic critical behavior of the three-dimensional bimodal random-field Ising model at the strong disorder regime. We present results in favor of the two-exponent scaling scenario, $\bar{\eta} = 2\eta$, where η and $\bar{\eta}$ are the critical exponents describing the power-law decay of the connected and disconnected correlation functions and we illustrate, using various finite-size measures and properly defined noise to signal ratios, the strong violation of self-averaging of the model in the ordered phase.

PACS. PACS. 05.50+q Lattice theory and statistics (Ising, Potts. etc.) – 64.60.De Statistical mechanics of model systems – 75.10.Nr Spin-glass and other random models

1 Introduction

Phase transitions in pure systems [1] are already well understood. The critical behavior of all physical quantities can be described via critical exponents which are related through (hyper)scaling relations to each other, so that only two independent exponents remain. In contrast, phase transitions in systems with (quenched) disorder [2] exhibit many puzzles and are still far from being understood. In statistical physics, and after the pioneering work of Imry and Ma [3], the random-field Ising model (RFIM) is a widely studied prototypical disordered system. It is believed [4,5] to be in the same universality class as the diluted antiferromagnet in a field, which can be studied experimentally [6].

Originally, it was believed [7,8,9] that the critical behavior of the d -dimensional RFIM is equal to that of the $d - 2$ pure ferromagnet, implying that the $d = 3$ RFIM exhibits no ordered phase. This is of course not true, as has been shown rigorously [10] a few years later [11]. In the meantime, a scaling theory [12,13,14] for the RFIM was developed, where the dimension d has been replaced by $d - \theta$ in the hyperscaling relations, θ being a third independent critical exponent, in contrast to the pure case. An alternative approach [15,16] leads to the consequence that θ is not independent but related to the exponent η via $\theta = 2 - \eta$ (two-exponent scaling scenario). Further evidence for the existence of only two independent exponents was found by high-temperature expansions [17]. This was mainly confirmed for the RFIM with a Gaussian random-field distribution in $d = 3$ by Monte Carlo (MC) simula-

tions [18] and exact ground-state calculations [19,20,21], and in $d = 4$ also by ground-state calculations [22]. The first goal of the present paper is the numerical verification of the above scenario for the case of the RFIM with a bimodal random-field distribution, yet having in mind that the precision of numerical simulations may never be good enough to actually prove that this scenario is truly verified; rather we should see this approach as a further test in favor of the proposed scaling picture of the RFIM. A first attempt towards this direction has been presented by Rieger and Young [23] in an early paper, yet their analysis was restricted to rather small lattice sizes ($L \leq 16$, L being the linear lattice dimension).

The second part of our study focuses on another important relevant issue in the study of disordered systems, that of self-averaging. Although it has been known for many years now that for (spin and regular) glasses there is no self-averaging in the ordered phase [24], for random ferromagnets such a behavior was first observed for the RFIM in a paper by Dayan *et al.* [25] and some years later for the random versions of the Ising and Ashkin-Teller models by Wiseman and Domany [26]. These latter authors suggested a finite-size scaling (FSS) ansatz describing the absence of self-averaging and the universal fluctuations of random systems near critical points that was refined and put on a more rigorous basis by the intriguing renormalization-group work of Aharony and Harris [27]. Ever since, the subject of breakdown of self-averaging is an important aspect in several theoretical and numerical investigations of disordered spin systems [28,29,30,31,32,33,34,35,36,37]. In fact, most recently, Efrat and Schwartz [39] showed that the property of lack of self-averaging in disordered systems may be turned into a useful tool that can provide an inde-

^a e-mail: nfyas@phys.uoa.gr

pendent measure to distinguish between the ordered and disordered phases of the system. In view of this increasing interest in the understanding of the self-averaging properties of disordered systems we attempt in the present paper to examine and apply the theoretical predictions to the RFIM, a suitable candidate which is already known to suffer from a strong violation of self-averaging in terms of the thermal properties [33,36].

The Hamiltonian describing the RFIM is

$$\mathcal{H} = -J \sum_{\langle i,j \rangle} S_i S_j - h \sum_i h_i S_i, \quad (1)$$

where S_i are Ising spins, $J > 0$ is the nearest-neighbors ferromagnetic interaction, h is the disorder strength, also called randomness of the system, and h_i are independent quenched random fields obtained here from a bimodal distribution of the form

$$P(h_i) = \frac{1}{2} [\delta(h_i - 1) + \delta(h_i + 1)]. \quad (2)$$

The critical value of h , denoted as critical disorder strength h_c , above which no phase transition occurs in the thermodynamic limit is known with good accuracy for the bimodal RFIM to be $h_c = 2.21(1)$ [19,40]. In particular, in the present paper we consider the model defined in equations (1) and (2) in the strong disorder regime ($h \in [1.9, 2.25]$) and embedded in simple cubic lattices with periodic boundary conditions and $N = L^3$ spins, where the linear dimension L takes values in the range $L = 4 - 32$. The ensembles of random-field realizations Q ($q = 1, 2, \dots, Q$) simulated for the present study are the following: $Q_{L \leq 16} = 1000$ and $Q_{L > 16} = 500$. The total computer time used for the simulations was several (~ 8) Intel Pentium-Pro months.

The rest of the paper is laid out as follows: In Section 2 we briefly describe here our numerical implementation, that is based on an efficient implementation of the Wang-Landau (WL) method [41], as also presented in a number of papers dealing with the simulation aspects of disordered systems [42,43,44]. In Section 3 we discuss the FSS behavior of the magnetic quantities of the model and provide evidence in favor of the two-exponent scaling scenario. Subsequently, in Section 4 we investigate the self-averaging properties of the model in terms of broad distributions and we illustrate using various finite-size measures and properly defined noise to signal ratios, the strong violation of self-averaging of the model in the ordered phase. Finally, we summarize our conclusions in Section 5.

2 Numerical approach

MC simulations in statistical physics now have a history of nearly half a century starting with the seminal work of Metropolis. While the Metropolis algorithm has been established as the standard algorithm for importance sampling it suffers from two problems: the inability to directly calculate the partition function, free energy or entropy,

and critical slowing down near phase transitions and in disordered systems. In a standard MC algorithm a series of configurations is generated according to a given distribution, usually the Boltzmann distribution in classical simulations. While this allows the calculation of thermal averages, it does not give the partition function, nor the free energy. They can only be obtained with limited accuracy as a temperature integral of the specific heat, or by using maximum entropy methods. The problem of critical slowing down has been overcome for second-order phase transitions by cluster update schemes [45]. For first-order phase transitions and systems with rough free-energy landscapes (such the present model under study) a decisive improvement was achieved some years ago via the WL algorithm [41].

In the last few years our group has used an entropic sampling implementation of the WL algorithm [41] to systematically study some simple [42], but also some more complex systems [36,40,43,44]. One basic ingredient of this implementation is a suitable restriction of the energy subspace for the implementation of the WL algorithm. This was originally termed as the critical minimum energy subspace (CrMES) restriction [42] and it can be carried out in many alternative ways, the simplest being that of observing the finite-size behavior of the tails of the energy probability density function (e-pdf) of the system [42].

Complications that may arise in complex systems, i.e. random systems or systems showing a first-order phase transition, can be easily accounted for by various simple modifications that take into account possible oscillations in the e-pdf and expected sample-to-sample fluctuations of individual realizations. In our recent papers [40,43,44], we have presented details of various sophisticated routes for the identification of the appropriate energy subspace (E_1, E_2) for the entropic sampling of each realization. In estimating the appropriate subspace from a chosen pseudocritical temperature one should be careful to account for the shift behavior of other important pseudocritical temperatures and extend the subspace appropriately from both low- and high-energy sides in order to achieve an accurate estimation of all finite-size anomalies. Of course, taking the union of the corresponding subspaces, insures accuracy for the temperature region of all studied pseudocritical temperatures.

The up to date version of our implementation uses a combination of several stages of the WL process. First, we carry out a starting (or preliminary) multi-range (multi-R) stage, in a very wide energy subspace. This preliminary stage is performed up to a certain level of the WL random walk. The WL refinement is $G(E) \rightarrow f \cdot G(E)$, where $G(E)$ is the density of states (DOS) and we follow the usual modification factor adjustment $f_{j+1} = \sqrt{f_j}$ and $f_1 = e$. The preliminary stage may consist of the levels: $j = 1, \dots, j = 18$ and to improve accuracy the process may be repeated several times. However, in repeating the preliminary process and in order to be efficient, we use only the levels $j = 13, \dots, 18$ after the first attempt, using as starting DOS the one obtained in the first random walk at the level $j = 12$. From our experience, this practice is almost equivalent to simulating the same number of

independent WL random walks. Also in our recent studies we have found out that is much more efficient and accurate to loosen up the originally applied very strict flatness criteria [42]. Thus, a variable flatness process starting at the first levels with a very loose flatness criteria and assuming at the level $j = 18$ the original strict flatness criteria is now days used. After the above described preliminary multi-R stage, in the wide energy subspace, one can proceed in a safe identification of the appropriate energy subspace using one or more alternatives outlined in reference [42].

The process continues in two further stages (two-stage process), using now mainly high iteration levels, where the modification factor is very close to unity and there is not any significant violation of the detailed balance condition during the WL process. These two stages are suitable for the accumulation of histogram data (for instance energy-magnetization histograms), which can be used for an accurate entropic calculation of non-thermal thermodynamic parameters, such as the order parameter and its susceptibility [42]. In the first (high-level) stage, we follow again a repeated several times (typically $\sim 5 - 10$) multi-R WL approach, carried out now only in the restricted energy subspace. The WL levels may be now chosen as $j = 18, 19, 20$ and as an appropriate starting DOS for the corresponding starting level the average DOS of the preliminary stage at the starting level may be used. Finally, the second (high-level) stage is applied in the refinement WL levels $j = j_i, \dots, j_i + 3$ (typically $j_i = 21$), where we usually test both an one-range (one-R) or a multi-R approach with large energy intervals. In the case of the one-R approach we have found very convenient and in most cases more accurate to follow the Belardinelli and Pereyra [46] adjustment of the WL modification factor according to the rule $\ln f \sim t^{-1}$, where t refers to the MC time of the process. Finally, it should be also noted that by applying in our scheme a separate accumulation of histogram data in the starting multi-R stage (in the wide energy subspace) offers the opportunity to inspect the behavior of all basic thermodynamic functions in an also wide temperature range and not only in the neighborhood of the finite-size anomalies.

Closing this review on the numerical part of this work, we would like to point out that, the above scheme may also be extended to accumulate multi-parametric histograms, and provide information for the critical properties of the system that are not easily accessible with other methodologies. For more details on this extension we refer the reader to reference [40].

3 Two-exponent scaling

We start by studying the critical behavior of the susceptibility χ and disconnected susceptibility χ_{dis} , which are given, in general, by the standard expressions

$$\chi = \frac{1}{NT} \sum_{i,j=1}^N (\langle S_i S_j \rangle - \langle S_i \rangle \langle S_j \rangle), \quad (3)$$

and

$$\chi_{dis} = \frac{1}{N} \sum_{i,j=1}^N \langle S_i \rangle \langle S_j \rangle, \quad (4)$$

where $\langle \dots \rangle$ denotes a thermal average. We now follow the scaling arguments based on the droplet theory [12,13,14], as presented by Dayan *et al.* [25]. According to these arguments, most samples in a large ensemble of realizations of the random field have only one thermally populated minimum. For these samples (called hereafter as typical) the two terms in equation (3) almost cancel at T_c , and while each term has separately the divergence of χ_{dis} , i.e.

$$\chi_{dis} \sim L^{4-\bar{\eta}} \quad (4 - \bar{\eta} = \bar{\gamma}/\nu), \quad (5)$$

their difference is given by

$$\chi_t \sim L^{2-\eta} \quad (2 - \eta = \gamma/\nu), \quad (6)$$

with probability $p_t \sim 1$ (the subscript t stands for typical). The cancellation of the most divergent terms in the expression of the susceptibility is rigorously true on average, according to the Schwartz-Soffer inequality [15]. Thus, following reference [15], one shows the inequality $4 - \bar{\eta} \leq d - 2\beta/\nu$, and assuming that this holds as an equality (see also reference [28]) one derives the modified hyperscaling relation

$$4 - \bar{\eta} = d - 2\beta/\nu, \quad (7)$$

which can be also written in the form

$$(d - \theta)\nu = 2\beta + \gamma. \quad (8)$$

The exponent θ in the above equation accounts for the violation of the hyperscaling relation and is given, according to the above equations (7) and (8), by

$$\theta = 2 - \bar{\eta} + \eta. \quad (9)$$

Furthermore, rare samples with more than one minimum (thermally populated) may appear with a probability $p_r \sim L^{-\theta}$ (where the subscript r stands for rare) and, for these samples, the two terms in equation (3) do not cancel at T_c , and their difference is of the same order of each term, i.e.

$$\chi_r \sim L^{4-\bar{\eta}}. \quad (10)$$

Although with increasing L the probability of obtaining one of these rare samples decreases, the susceptibility of a rare sample gets much larger, relatively to the value of a typical sample ($\chi_r \gg \chi_t$, see Figure 1). Thus, we need to average over large ensembles of random fields in order to obtain good statistics.

Averaging over Q realizations of the random field and using equations (6) and (10), we see that for the first moment $[\chi]_{av}$ (where $[\dots]_{av}$ denotes randomness averaging), both typical and rare samples give a comparable contribution, so that at T_c

$$[\chi]_{av} = \sum_{i=t,r} p_i \chi_i \sim 1 \cdot L^{2-\eta} + L^{-\theta} \cdot L^{4-\bar{\eta}} \sim L^{2-\eta}. \quad (11)$$

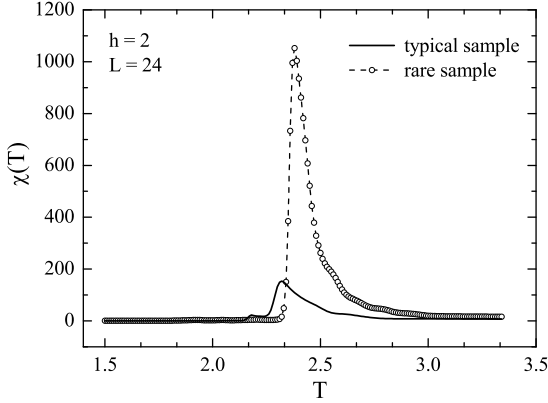


Fig. 1. Magnetic susceptibility as a function of temperature of a typical (solid line) and a rare (dotted line) sample for $h = 2$ and $L = 24$.

The behavior of the average disconnected susceptibility at T_c is, according to equation (5),

$$[\chi_{dis}]_{av} \sim L^{4-\bar{\eta}}. \quad (12)$$

At this point we shall assume that the above power laws are valid also for the pseudocritical temperatures of some relevant thermodynamic quantities. In particular, we will consider here (mainly) the sequence of pseudocritical temperatures that correspond to the maxima (for different L) of the average susceptibility ($[\chi]_{av}^*$) defined as

$$[\chi]_{av}^* = \max_T \{[\chi]_{av}\} = \max_T \left\{ \frac{1}{Q} \sum_{q=1}^Q \chi_q(T) \right\}, \quad (13)$$

where the subscript q refers to a particular random realization of the quenched disorder and χ_q to the corresponding magnetic susceptibility. These pseudocritical temperatures will be denoted in the sequel as $T_{L,[\chi]_{av}^*}$ (for the case of the specific heat the corresponding pseudocritical temperatures will be denoted as $T = T_{L,[C]_{av}^*}$). In Figure 2(a) we plot the maxima of the average susceptibility versus the lattice size L in a log-log plot for the case $h = 2$. The full line is a least-squares straight-line fitting which gives a slope of 1.49(2), that is according to equation (11) an estimate for $2 - \eta$, yielding

$$\eta = 0.51(2). \quad (14)$$

The average disconnected susceptibility at $T_{L,[\chi]_{av}^*}$, denoted as $[\chi_{dis}]_{av}^*$, is depicted in Figure 2(b), also for $h = 2$, and is expected to obey the power law (12). Using again a least-squares fitting of the data to a straight line in the log-log plot we get the estimate for $4 - \bar{\eta}$ to be 2.99(3), and therefore

$$\bar{\eta} = 1.01(3). \quad (15)$$

From equations (14) and (15) we see that the Schwartz-Soffer inequality $\bar{\eta} \leq 2\eta$ [15] is fulfilled within error bars as an equality, supporting the two-exponent scaling scenario,

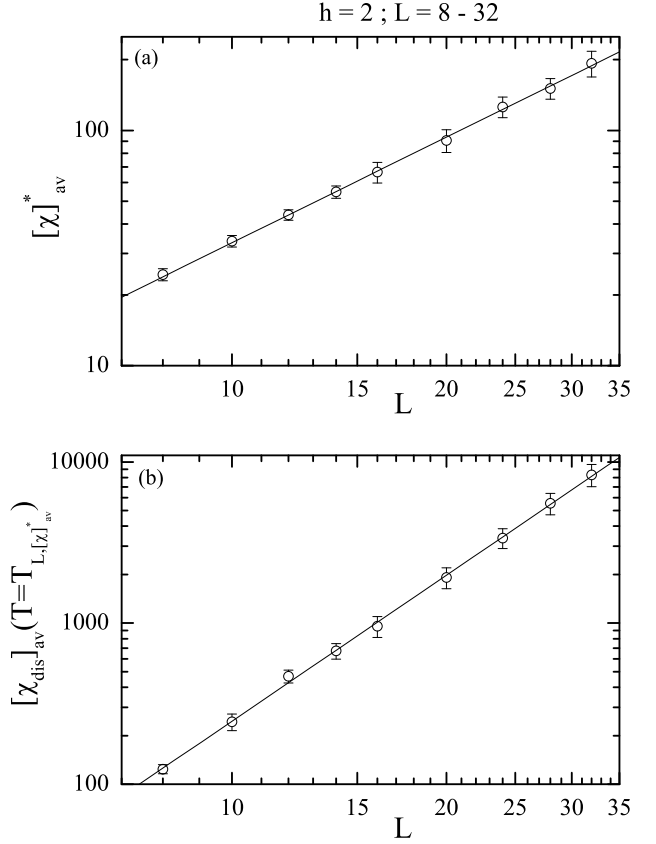


Fig. 2. FSS in a double-logarithmic scale of (a) the maxima of the average susceptibility and (b) the average disconnected susceptibility at the temperature where the average susceptibility attains its maximum, for $h = 2$ and $L = 8 - 32$. In both panels the solid lines show linear fitting attempts.

i.e. $\bar{\eta} = 2\eta$ [17,15,16]. The exponent θ is estimated from equation (9) to be

$$\theta = 1.50(3). \quad (16)$$

Overall, the estimated values for η , $\bar{\eta}$, and θ are in very close agreement with the values

$$\eta = 0.5 \quad \bar{\eta} = 1 \quad \theta = 1.5, \quad (17)$$

that can be predicted from elementary considerations in the ordered phase (see also the discussion in reference [25]) and agree with the early dimensional reduction prediction $d \rightarrow d/2$ of Shapir [47]. Moreover, the resulting value for the exponent β is very close to zero, as already noted by Dayan *et al.* [25]. The resulting very small value for β ($\beta = 0.007(5)$) with a relatively large error could be compared with renormalization group results ($\beta = 0.0200(5)$) [48] and zero temperature studies ($\beta = 0.017(5)$) [21].

Up to this point, our analysis and discussion followed the assumption of a continuous phase transition, which is

actually the most widely accepted scenario in the random-field community. However, the estimated value for the critical exponent β raises some doubts of whether this is actually true, especially for the present case of the bimodal RFIM, for which mean-field theory predicted a tricritical point at high values of the random field [49]. This main issue has regained interest after the recent observations, in both the bimodal [50,51] and Gaussian [37,52] cases, of first-order-like features at the strong disorder regime. In particular first-order-like features, such as the appearance of the characteristic double-peak structure of the canonical e-pdf, have been recently reported for both the Gaussian and the bimodal distributions of the $d = 3$ RFIM.

However, in a recent paper Fytas et al. [43] presented a detailed study of the first-order transition features - in terms of the surface tension and latent heat - of the $d = 3$ RFIM, having in mind that a mere observation of a first-order structure is not sufficient for the identification of the transition. As it was shown in reference [43], this is especially true for the RFIM, since its critical behavior is obscured by strong and complex finite-size effects, involving also the important issue of the lack of self-averaging, discussed here in the next Section. The results of reference [43] for two values of the disorder strength in the strong disorder regime ($h = 2$ and $h = 2.25$) clearly indicated that the interface tension vanishes and the two peaks of the e-pdf move together in the thermodynamic limit and therefore provided convincing evidence that the transition is continuous and that there is no tricritical point along the phase transition line. These results pointed to an unconventional continuous transition, in which the e-pdf approaches two delta functions that move together in the thermodynamic limit. Such an unconventional behavior has been originally predicted by Eichhorn and Binder [28], for the order-parameter pdf of the $d = 3$ random-field three-state Potts model and found its theoretical justification in the framework of a refined FSS theory a few months ago in a profound paper by Vink et al. [53].

Closing this Section, we may also calculate the critical exponents γ of the susceptibility and $\bar{\gamma}$ of the disconnected susceptibility

$$\begin{aligned}\gamma &= \nu(2 - \eta) = 1.95(27) \\ \bar{\gamma} &= \nu(4 - \bar{\eta}) = 3.92(54),\end{aligned}\quad (18)$$

which also compare favorably with previous estimations [25,23,17,18,20]. Note that in equation (18) the large error bounds come mainly from the error bounds in ν , since we have used the value $\nu = 1.31(18)$ estimated in our previous work [36]. We would like to note here that, an analogous study of χ and χ_{dis} was performed by Eichhorn and Binder [28] for the $d = 3$ three-state random-field Potts model. Their findings provided also qualitative evidence for the two-exponent scaling description of random-field systems.

4 Broad distributions and lack of self-averaging

Let us start this Section by recapitulating some basic definitions and concepts on self-averaging. As discussed above,

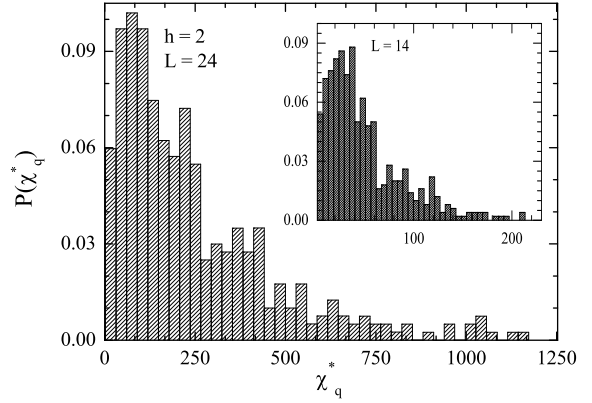


Fig. 3. The histograms for the probability distribution $P(\chi_q^*)$ of the susceptibility maxima for $L = 24$ (and $L = 14$ in the inset).

our numerical studies of disordered systems are carried out near their critical points using finite samples; each sample q is a particular random realization of the quenched disorder. A measurement of a thermodynamic property w yields a different value for the exact thermal average w_q of every sample q . In an ensemble of disordered samples of linear size L the values of w_q are distributed according to a probability distribution $P(w_q)$. The behavior of this distribution is directly related to the issue of self-averaging. In particular, by studying the behavior of the width of $P(w_q)$ with increasing the system size L , one may address qualitatively the issue of self-averaging, as has already been stressed by previous authors [30]. In general, we characterize the distribution $P(w_q)$ by its average $[w]_{av}$ and also by the relative variance

$$R_w = \frac{V_w}{[w]_{av}^2} = \frac{[w^2]_{av} - [w]_{av}^2}{[w]_{av}^2}. \quad (19)$$

Suppose now that w is a singular density of an extensive thermodynamic property, such as M or χ , or the singular part of $e(= E/N)$ and C . The system is said to exhibit self-averaging if $R_w \rightarrow 0$ as $L \rightarrow \infty$. If R_w tends to a non-zero value, i.e. $R_w \rightarrow const \neq 0$ as $L \rightarrow \infty$, then the system exhibits lack of self-averaging.

The importance of the above concepts has been illustrated by Aharony and Harris [27] and their main conclusions are summarized as follows: (i) Outside the critical temperature: $R_w = 0$. In a finite geometry, the correlation length ξ is finite for $T \neq T_c$ and it can be found, using general statistical arguments, originally introduced by Brout [54], that $R_w \propto (\xi/L)^d \rightarrow 0$, as $L \rightarrow \infty$. This is called strong self-averaging. (ii) At the critical temperature there exist two possible scenarios: (a) models in which according to the Harris criterion [55] the disorder is relevant ($\alpha_p > 0$): $R_w \neq 0$. Then, the system at the critical point is not self-averaging and (b) models in which according to the Harris criterion disorder is irrelevant ($\alpha_p < 0$): $R_w = 0$. In this case R_w scales as $L^{\alpha/\nu}$,

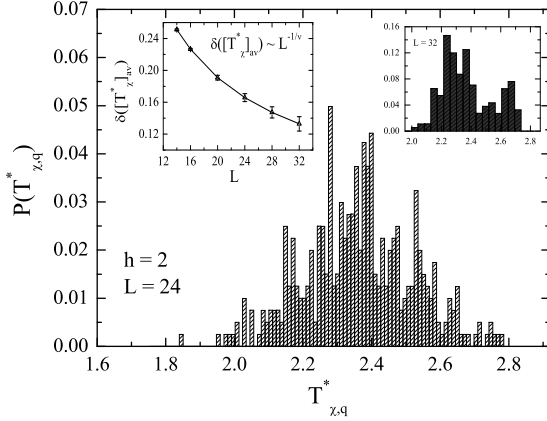


Fig. 4. The $h = 2$ histograms of the probability distribution $P(T_{\chi,q}^*)$ for $L = 24$ (main panel) and $L = 32$ (right inset). The left inset shows the FSS of the sample-to-sample variance of the average $[T_{\chi}^*]_{av}$.

where α and ν are the critical exponents of the pure system, which are the same in the disordered one. This is called weak self-averaging. (iii) The pseudocritical temperatures $T_{w,q}^*$ of the disordered system are distributed with a width $\delta([T_w^*]_{av})$ which scales with the system size as $\delta([T_w^*]_{av}) \sim L^{-n}$, where $n = d/2$ or $n = 1/\nu$, depending on whether the disordered system is controlled by the pure or the random fixed point, respectively. The above behavior is now well established by the pioneering works of Aharony and Harris [27] and Wiseman and Domany [26,30].

We start the presentation of our results with the probability distribution of the susceptibility maxima $P(\chi_q^*)$. $P(\chi_q^*)$ is expected to be a broad distribution with a most probable value of the order $L^{2-\eta}$ and a tail extending to much larger values of the order $L^{4-\bar{\eta}}$ [25]. Figure 3 and the corresponding inset show the normalized histograms of $P(\chi_q^*)$ at $h = 2$ for lattice sizes $L = 24$ and $L = 14$, respectively. In both cases $P(\chi_q^*)$ has its peak at a rather small value of χ_q^* but there is a clearly developing long tail extending to much larger values of χ_q^* . As expected, the tail is longer for the larger lattice size. Subsequently, in the main panel and right inset of Figure 4 we plot the $h = 2$ histograms for the probability distribution $P(T_{\chi,q}^*)$ of the pseudocritical temperatures of the magnetic susceptibility for $L = 24$ and $L = 32$, respectively. The left inset in Figure 4 illustrates the scaling of the sample-to-sample variance of the sample average

$$[T_{\chi}^*]_{av} = (1/Q) \sum_{q=1}^Q T_{\chi,q}^*. \quad (20)$$

Assuming that the width of these sample-to-sample fluctuations scales with the linear size L according to

$$\delta([T_{\chi}^*]_{av}) \sim L^{-1/\nu}, \quad (21)$$

we obtain, from the very good fitting for the sizes $L = 14 - 32$ shown in the inset of Figure 4, the value $\nu =$

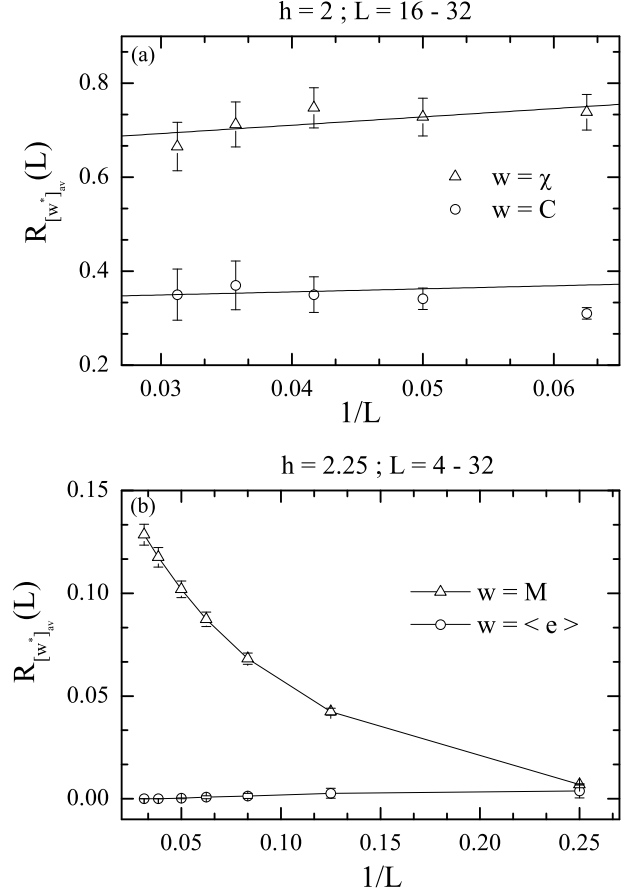


Fig. 5. FSS behavior of the ratio $R_{[w^*]_{av}}(L)$ defined in equation (22) for (a) the specific heat $w = C$ and magnetic susceptibility $w = \chi$ for $h = 2$ and (b) the magnetization $w = M$ and the mean energy per spin $w = \langle e \rangle$ for $h = 2.25$. In panel (a) the solid lines show linear fitting extrapolations to the limit $L \rightarrow \infty$.

1.30(2). This estimate is in excellent agreement with the value $\nu = 1.31(18)$ used in equation (18) and estimated in our previous paper [36] from the scaling of the specific heat's pseudocritical temperature and consists further evidence for the breakdown of self-averaging in the RFIM.

We turn now to study the behavior of the ratio R_w defined above. In our formalism, we may define the variance ratio R_w in two distinct forms. One L -dependent ratio for the sample average of the individual maxima of w $[w^*]_{av} = (1/Q) \sum_{q=1}^Q w_q^*$

$$R_{[w^*]_{av}}(L) = \frac{V_{[w^*]_{av}}}{[w^*]_{av}^2}, \quad (22)$$

and one T -dependent for the average curve $[w]_{av}$

$$R_{[w]_{av}}(T) = \frac{V_{[w]_{av}}}{[w]_{av}^2}. \quad (23)$$

In Figure 5(a) the behavior of the ratio $R_{[w^*]_{av}}(L)$, defined in equation (22), where $w^* = \chi^* = \chi(T = T_{L,[\chi]_{av}}^*)$ and

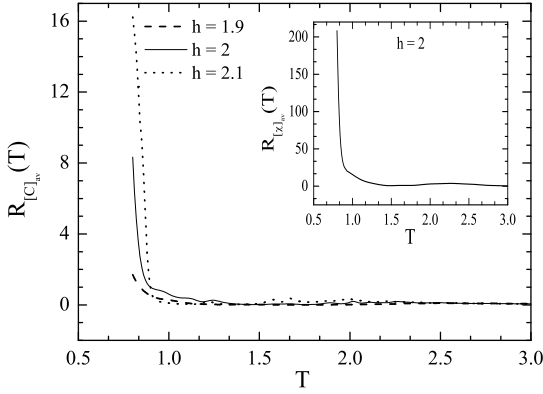


Fig. 6. Low-temperature behavior of the ratio $R_{[w]_{av}}(T)$ defined in equation (23) of the specific heat ($w = C$) and $h = 1.9, 2$, and 2.1 in the main panel and the magnetic susceptibility ($w = \chi$) and $h = 2$ in the corresponding inset. The linear size dimension is $L = 10$.

$w^* = C^* = C(T = T_{L,[C]_{av}}^*)$ is illustrated for $L = 16 - 32$, as a function of the inverse linear size for disorder strength $h = 2$. The straight lines are extrapolations to $L \rightarrow \infty$. In both cases a clear saturation to a non-zero limiting value is observed, i.e. $\lim_{L \rightarrow \infty} R_{[\chi^*]_{av}}(L) = 0.64(9)$ and $\lim_{L \rightarrow \infty} R_{[C^*]_{av}}(L) = 0.33(5)$, indicating violation of self-averaging [36,27,30,39]. For the case of the susceptibility this violation is much stronger. Figure 5(b) presents the behavior of the ratio $R_{[w^*]_{av}}(L)$, where now $w^* = M^* = M(T = T_{L,[\chi]_{av}}^*)$ and $w^* = \langle e \rangle^* = \langle e \rangle(T = T_{L,[C]_{av}}^*)$ as a function of the inverse linear size for sizes $L = 4 - 32$ and disorder strength $h = 2.25$. It is clear that, while for the magnetization the ratio $R_{[M^*]_{av}}(L)$ approaches a non zero value in the limit $L \rightarrow \infty$ and therefore violation of self-averaging is expected, the same ratio for the mean energy $R_{[\langle e \rangle^*]_{av}}(L)$ starts with some very small values but finally approaches zero with increasing lattice size, indicating that in the infinite size limit the mean energy of the system is self-averaging.

Finally, in Figure 6 we present the low-temperature behavior of the ratio $R_{[w]_{av}}(T)$, defined in equation (23), for the specific heat $w = C$ and the susceptibility $w = \chi$ (inset) at $h = 2$ and for a lattice size $L = 10$. The ratio $R_{[C]_{av}}$ for $h = 1.9$ and $h = 2.1$ is also shown in the main panel together with that of $h = 2$, calculated via the extrapolation scheme described in reference [40]. Our intention is to identify the temperature variation of the non self-averaging property of the average specific heat and susceptibility. We observe that as we move from the disordered phase to the ordered phase this ratio increases, and gets its maximum value for the lowest temperatures shown. This indicates strong sample-to-sample fluctuations and non self-averaging behavior (which is more pronounced with increasing disorder strength), it becomes more evident as we enter the ordered phase, and is in agreement with previous studies [25,23,18]. Since the sample-averaged pseudocritical temperature for $L = 10$ is of the order of $[T_{\chi}^*]_{av} \simeq$

2.7, the violation of self-averaging goes well into the ordered phase, and this should be compared with Figure 3 of reference [39].

Let us comment here that, as stated above, possible breakdown of self-averaging may be traced back to situations where the correlation length ξ becomes of the order of the linear size of the system. The usual state of affairs is that the correlation length diverges just on the boundary between the ordered and disordered phase and consequently any break down of self-averaging may be observed only in the vicinity of the boundary [36,27,30,39]. However, as Dayan et al. [25] showed, the situation in the RFIM is quite different: the correlation length is of order of the linear size of the system everywhere in the ordered phase and not just at the boundary of the phase, indicating a violation of self-averaging in the ordered phase, as clearly manifested in our Figure 6. Of course, self-averaging is expected to be restored at high-temperatures (above T_c) that $\xi \ll L$, because in this case, the system can be divided into independent regions of size ξ and any measurement on the whole sample will be an average on these regions. This latter behavior is also depicted in our Figure 6, where the ratio decreases rapidly and approaches zero for high temperatures for both the specific heat and the susceptibility.

5 Conclusions

In the present paper we investigated numerically some important aspects of the critical properties of the $d = 3$ RFIM with a bimodal random-field distribution in the strong disorder regime. In the first part of our study we focused on the scaling aspects of the model and presented evidence in favor of the so-called two-exponent scaling scenario. We also derived accurate values for the magnetic critical exponents β , γ , and $\bar{\gamma}$ of the model in good agreement with the existing estimates in the literature.

In the second part, we investigated the self-averaging properties of the model in terms of probability distributions of certain thermodynamic quantities and we illustrated, using various finite-size measures and properly defined noise to signal ratios, the strong violation of self-averaging of the model in the ordered phase. Additionally, a FSS analysis of the width of the distribution of the sample-dependent pseudocritical temperatures of the magnetic susceptibility verified the theoretical expectations of Aharony and Harris and provided an alternative approach of extracting the value of the correlation length's exponent ν . Overall, the data and analysis presented in this paper indicate that the most complicated issue of breakdown of self-averaging in disordered systems deserves special attention and can be easily transformed into a useful tool that constitutes an alternative approach to criticality.

References

1. J. Cardy, *Scaling and Renormalization in Statistical Physics*, (Cambridge University Press 1996)

2. A.P. Young (ed.), *Spin glasses and random fields*, (World Scientific, Singapore 1998)
3. Y. Imry, S.-K Ma, Phys. Rev. Lett. **35**, 1399 (1975)
4. S. Fishman, A. Aharony, J. Phys. C **12**, L729 (1979)
5. J.L. Cardy, Phys. Rev. B **29**, 505 (1984)
6. D.P. Belanger, in: A.P. Young (ed.), *Spin Glasses and Random Fields*, (World Scientific, Singapore 1998)
7. A. Aharony, Y. Imry, S.-K. Ma, Phys. Rev. Lett. **37**, 1364 (1976)
8. A.P. Young, J. Phys. C **10**, L257 (1977)
9. G. Parisi, N. Sourlas, Phys. Rev. Lett. **43**, 744 (1979)
10. J. Bricmont, A. Kupiainen, Phys. Rev. Lett. **59**, 1829 (1987)
11. Although reference [10] triggered most recent studies on the $d = 3$ RFIM, several very interesting studies of the static and dynamic properties of $d = 2$ random-field systems exist, see for example: E.T. Seppälä, M.J. Alava, Phys. Rev. E **63**, 066109 (2001); E.T. Seppälä, M.J. Alava, I.J. Sillanpää, J. Magn. Magn. Mater. **272**, 1286 (2004)
12. J. Villain J. Physique **46**, 1843 (1985)
13. A.J. Bray, M.A. Moore, J. Phys. C **18**, L927 (1985)
14. D.S. Fisher, Phys. Rev. Lett. **56**, 416 (1986)
15. M. Schwartz, A. Soffer, Phys. Rev. Lett. **55**, 2499 (1985)
16. M. Schwartz, J. Phys. C **18**, 135 (1985); M. Schwartz, A. Soffer, Phys. Rev. B **33**, 2059 (1986); M. Schwartz, M. Gofman, T. Nattermann, Physica A **178**, 6 (1991); M. Schwartz, Europhys. Lett. **15**, 777 (1994)
17. M. Gofman, J. Adler, A. Aharony, A.B. Harris, M. Schwartz, Phys. Rev. Lett. **71**, 1569 (1993)
18. H. Rieger, Phys. Rev B **52**, 6659 (1995)
19. A.K. Hartmann, U. Nowak, Eur. Phys. J. B **7**, 105 (1999)
20. A.K. Hartmann, A.P. Young, Phys. Rev. B **64**, 214419 (2001)
21. A.A. Middleton, D.S. Fisher, Phys. Rev. B **65**, 134411 (2002)
22. A.K. Hartmann, Phys. Rev. B **65**, 174427 (2002)
23. H. Rieger, A.P. Young, J. Phys. A **26**, 5279 (1993)
24. K. Binder, A.P. Young, Rev. Mod. Phys. **58**, 837 (1986)
25. I. Dayan, M. Schwartz, A.P. Young, J. Phys. C **26**, 3093 (1993)
26. S. Wiseman, E. Domany, Phys. Rev. E **52**, 3469 (1995)
27. A. Aharony, A.B. Harris, Phys. Rev. Lett. **77**, 3700 (1996)
28. K. Eichhorn, K. Binder, J. Phys. C **8**, 5209 (1996)
29. F. Pázmándi, R. Scalettar, G.T. Zimányi, Phys. Rev. Lett. **79**, 5130 (1997)
30. S. Wiseman, E. Domany, Phys. Rev. Lett. **81**, 22 (1998)
31. H.G. Ballesteros, L.A. Fernández, V. Martín-Mayor, A. Muñoz Sudupe, G. Parisi, J.J. Ruiz-Lorenzo, Phys. Rev. B **58**, 2740 (1998)
32. Y. Tomita, Y. Okabe, Phys. Rev. E **64**, 036114 (2001)
33. G. Parisi, N. Sourlas, Phys. Rev. Lett. **89**, 257204 (2002)
34. P.E. Berche, C. Chatelain, B. Berche, W. Janke, Eur. Phys. J. B **38**, 463 (2004)
35. C. Monthus, T. Garel, Eur. Phys. J. B **48**, 393 (2005)
36. A. Malakis, N.G. Fytas, Phys. Rev. E **73**, 016109 (2006)
37. Y. Wu, J. Machta, Phys. Rev. B **74**, 064418 (2006)
38. A. Gordillo-Guerrero, J.J. Ruiz-Lorenzo, J. Stat. Mech.: Theory Exp. (2007) P0601
39. A. Efrat, M. Schwartz, arXiv:cond-mat/0608435
40. N.G. Fytas, A. Malakis, Eur. Phys. J. B **61**, 111 (2008)
41. F. Wang, D. P. Landau, Phys. Rev. Lett. **86**, 2050 (2001); Phys. Rev. E **64**, 056101 (2001)
42. A. Malakis, A. Peratzakis, N.G. Fytas, Phys. Rev. E **70**, 066128 (2004); A. Malakis, S.S. Martinos, I.A. Hadjiagapiou, N.G. Fytas, P. Kalozoumis, Phys. Rev. E **72**, 066120 (2005)
43. N.G. Fytas, A. Malakis, K. Eftaxias, J. Stat. Mech.: Theory Exp. (2008) P03015
44. A. Malakis, A.N. Berker, I.A. Hadjiagapiou, N.G. Fytas, Phys. Rev. E **79**, 011125 (2009); A. Malakis, A.N. Berker, I.A. Hadjiagapiou, N.G. Fytas, T. Papakonstantinou, Phys. Rev. E **81**, 041113 (2010) R.H.
45. R.H. Swendsen, J.-S. Wang, Phys. Rev. Lett. **58**, 86 (1987); U. Wolff, Phys. Rev. Lett. **62**, 361 (1989)
46. R.E. Belardinelli, V.D. Pereyra, Phys. Rev. E **75**, 046701 (2007)
47. Y. Shapir, Phys. Rev. Lett. **54**, 154 (1985)
48. A. Falicov, A.N. Berker, S.R. McKay, Phys. Rev. B **51**, 8266 (1995)
49. A. Aharony, Phys. Rev. B **18**, 3318 (1978); A. Aharony, Phys. Rev. B **18**, 3328 (1978)
50. L. Hernández, H.T. Diep, Phys. Rev. B, **55** 14080 (1997)
51. L. Hernández, H. Ceva, Physica A **387**, 2793 (2008)
52. A. Maiorano, V. Martín-Mayor, J.J. Ruiz-Lorenzo, A. Tarancón, Phys. Rev. B **76**, 064435 (2007)
53. R.L.C. Vink, T. Fischer, K. Binder, arXiv:cond-mat/0608435
54. R. Brout, Phys. Rev. **115**, 824 (1959)
55. A.B. Harris, J. Phys. C **7**, 1671 (1974)